Seismological Research Letters, Volume 63, No. 2, April - June, 1992

A STUDENT'S GUIDE TO TELESEISMIC BODY WAVE AMPLITUDES

Emile A. Okal

Department of Geological Sciences
Northwestern University,
Evanston, Illinois 60208

ABSTRACT

We discuss the nature of the various factors contributing to the amplitude of a teleseismic body wave in the context of a geometrical ray solution, specifically: the radiation of elastic waves into an elastic medium by a point source; the radiation patterns resulting from the orientation of the double-couple in space; the effect of propagation through a radially heterogeneous Earth, known as geometrical spreading; the effect of anelastic attenuation; the contribution of depth phases to the seismogram; and finally the influence of distance on the receiver response function. For each of these parameters, we emphasize the physical arguments underlying the exact algebraic expressions of the various factors contributing to the seismic amplitude. Finally, we discuss the extension of the geometrical ray solution to deep seismic sources.

INTRODUCTION

The problem of calculating the amplitude of a teleseismic body wave in a laterally homogeneous Earth, as generated by a dislocation of known geometry, has long been studied and adequate algorithms published in the literature. We refer for example to the Cagniard–de Hoop method (Helmberger, 1968), the reflectivity method (Fuchs and Müller, 1971), and the generalized ray theory (Chapman, 1978).

A simple and reasonably accurate algorithm is the so-called geometrical ray solution, as described for example in Chapter 4 of Aki and Richards' (1980) textbook (hereafter AR80). While this method has significant limitations (for example, it cannot be applied at the turning point of a ray, nor can it handle caustics), it allows the computation of long-period synthetic waveshapes of a quality acceptable in many seismological problems.

This algorithm has evolved from such works as Langston and Helmberger's (1975) and Kanamori and Stewart's (1976; hereafter KS76). While the formulæ published in the original research papers are of course correct, they occasionally derive from rather intricate theories, and the format of their publication was not geared to a didactic discussion of their physical meaning. The purpose of the present paper is therefore to review the various terms involved in the amplitude of a teleseismic body wave, and to present a discussion of their individual contributions, in the hope of clarifying their physical origin, and of shedding some light on a matter which, because of the intrinsic complexity of the underlying theories, may occasionally appear confusing.

Specifically, we start with KS76's Equation (8), giving the teleseismic amplitude of a P wave resulting from a shear dislocation. We wish to discuss all the terms on the basis of simple physical arguments. We rewrite the equation in the slightly different notation

$$u^P(\Delta, \phi;\ t) = \frac{M_0}{4\pi\rho_h\alpha_h^3} \cdot \frac{g(\Delta)}{a} \cdot \Big[R^P\ \dot{X}(t - \tau^P) + R^{pP} \cdot \Pi^{PP}(i_h)\ \dot{X}(t - \tau^{pP}) + R^{sP} \cdot \frac{\alpha_h \cos i_h}{\beta_h \cos j_h}\ \Pi^{SP}(j_h)\ \dot{X}(t - \tau^{sP}) \Big] \cdot C^P(i_0) * Q(t, Q^P, \tau^P) * I(t) \qquad (1)$$

Here, we write the source time function as $X(t)$, and the travel times of P, pP and sP as τ^P, τ^{pP} and τ^{sP} respectively. In general, we will write an incidence angle as i for a P–type ray, and j for an S–type ray. The subscript h relates to angles (or characteristic material properties) at the source depth h. The asterisk represents the convolution operator.

Equation (1) outlines that the amplitude of a teleseismic wave is controlled in very general terms by:

- the amplitude radiated in the immediate vicinity of the source by the particular double-

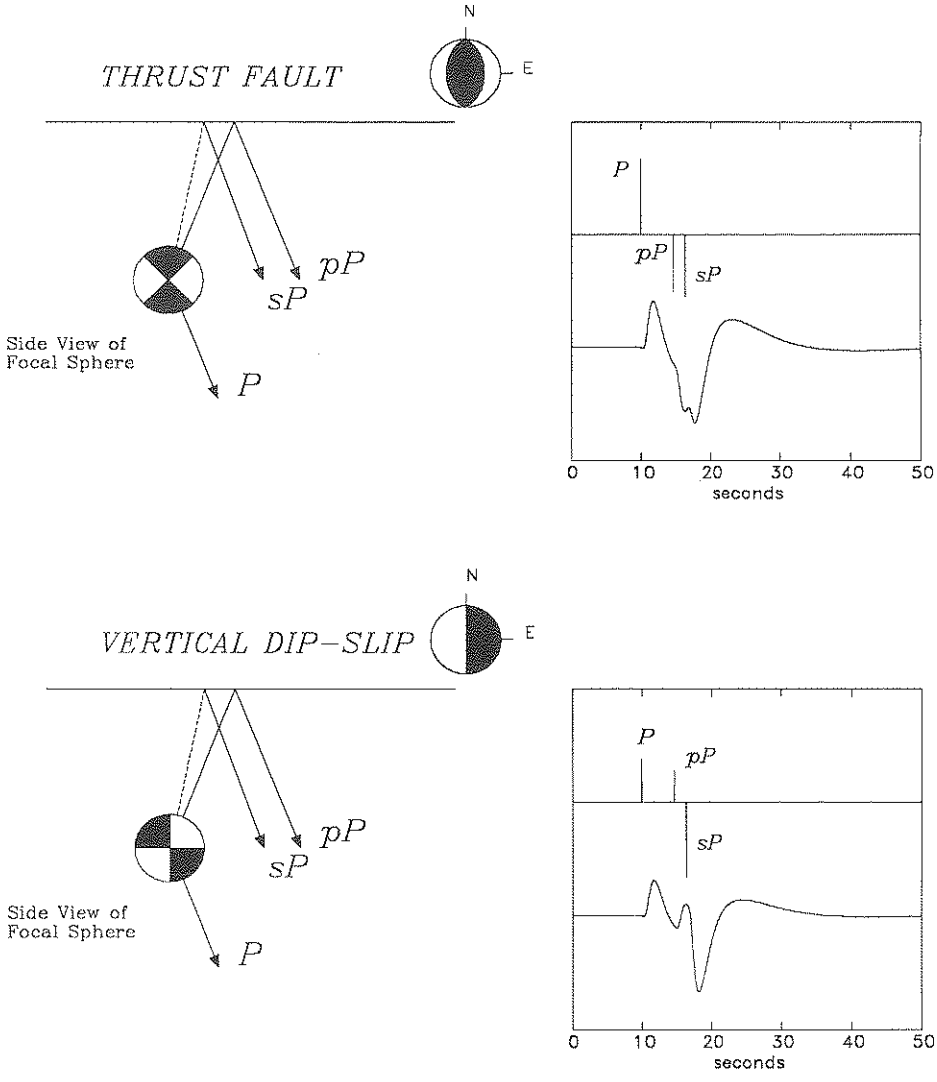

Fig. 1. Examples of the combination of the phases P, pP and sP into the generalized P wave at teleseismic distances. A simple, homogeneous half-space is assumed, and the station is due East of the event. Each mechanism is identified (next to the title) by its familiar beachball. The geometry of the rays departing the source is given on the left diagrams in relation to the focal sphere, represented as seen sideways, looking North at the source depth. The diagrams on the right show the relative contribution of direct P and the reflected phases. The top traces involve only the source excitation and reflection at the surface; the bottom ones involve geometrical spreading, anelastic attenuation, and convolution with a WWSSN Long-Period instrument. Note that in the thrust case, pP is initially of the same polarity as P, but ends up reversed by the reflection, while in the dip-slip case, pP is initially reversed, and ends up of the same polarity as P, resulting in a significantly different waveshape. (After S. Stein, manuscript in preparation).

couple involved: $\frac{M_0}{4\pi\rho_h\alpha_h^3} R^P \dot{X}(t-\tau^P)$, where M_0 is the seismic moment of the source with time dependence $X(t)$, R^P a radiation coefficient, and ρ_h and α_h the density and P-wave velocity at the source;

- the effect of the propagation through the elastic solid Earth, known as geometrical spread-

ing: $\frac{g(\Delta)}{a}$, where a is the Earth's radius;

- the effect of attenuation due to the Earth's anelasticity expressed through the convolution with the attenuation operator Q;
- the response of the receiving site (C^P) to a ray incident at the angle i_0 ; and that of the instrument, expressed through convolution with the instrument operator $I(t)$, which we will not discuss here.

In addition, a teleseismic arrival from a shallow source usually includes the reflected phases, for example pP and sP in the case of a teleseismic P wave (see Figure 1); their contribution, normalized to that of direct P is detailed inside the bracket in (1), where β_h is the S–wave velocity at the source, and the coefficients Π are reflection coefficients at the Earth's surface. Later sections will justify the amplitudes of the reflected phases, and will discuss the application of the formalism to deep earthquakes.

EXCITATION AT THE SOURCE

In the immediate vicinity of the hypocenter, the medium can be regarded as homogeneous and infinite, and the problem is simply that of its response to a double-couple of time dependence $X(t)$, as detailed in Chapter 4 of AR80. The seismic displacement in the far field is given by their Equation (4.87) which can be written in a slightly different notation

$$\begin{aligned} \mathbf{u}^P &= \frac{R^P}{4\pi\rho\alpha^3}\,\frac{M_0}{r}\,\dot{X}(t-\frac{r}{\alpha})\,\hat{\mathbf{l}} \\ \mathbf{u}^{SV} &= \frac{R^{SV}}{4\pi\rho\beta^3}\,\frac{M_0}{r}\,\dot{X}(t-\frac{r}{\beta})\,\hat{\mathbf{p}} \\ \mathbf{u}^{SH} &= \frac{R^{SH}}{4\pi\rho\beta^3}\,\frac{M_0}{r}\,\dot{X}(t-\frac{r}{\beta})\,\hat{\boldsymbol{\phi}} \end{aligned} \qquad (2)$$

where, for simplicity, we have dropped the subscripts h. In addition r is the distance to the source, and the frame $\hat{\mathbf{l}}$, $\hat{\mathbf{p}}$, $\hat{\boldsymbol{\phi}}$ is described on Figure 2, adapted from Figure 4.20 of AR80.

These equations are worthy of comment. The factor $\rho\alpha^3$ (for P; $\rho\beta^3$ for S) in the denominator can be explained physically by splitting it into $(\rho\alpha^2)\alpha$. The first factor is nothing but the appropriate elastic modulus (or combination of the elastic moduli K and μ) expressing the response of the medium to a dynamic point force. Combinations of K and μ are similarly present in all components of the static Somigliana tensor (which is the solution to a classic problem in Elasticity: what is the vector displacement u at a point x in space due to a point force f at the origin x_0?). The additional factor $1/\alpha$ or $1/\beta$ is introduced when going from a single force to a double-couple. The field created by a couple (or double-couple) is fundamentally the spatial derivative of that of a force. In the far field, the spatial variation is primarily due to the propagation of the time history of the source at the velocity α, hence the factor $1/\alpha$, which goes hand in hand with the time derivative $\dot{X}$ of the source time function.

An immediate consequence of the presence of the cube of the intrinsic hypocentral velocity in the denominator is the well known observation that teleseismic S waves are of significantly larger amplitude than P waves (in principle $3\sqrt{3}$ or about 5 times at periods long enough not to be affected by anelastic attenuation; see below).

RADIATION PATTERNS

The expression of the radiation patterns R^P, R^{SV}, R^{SH} of body waves by double-couples has been given in a variety of notations, including in KS76 and AR80. It is important to note that the orientation conventions of KS76 and AR80 are different. Both authors orient $\mathbf{u}^P$ positive in the direction of propagation (positive upwards upon reach-

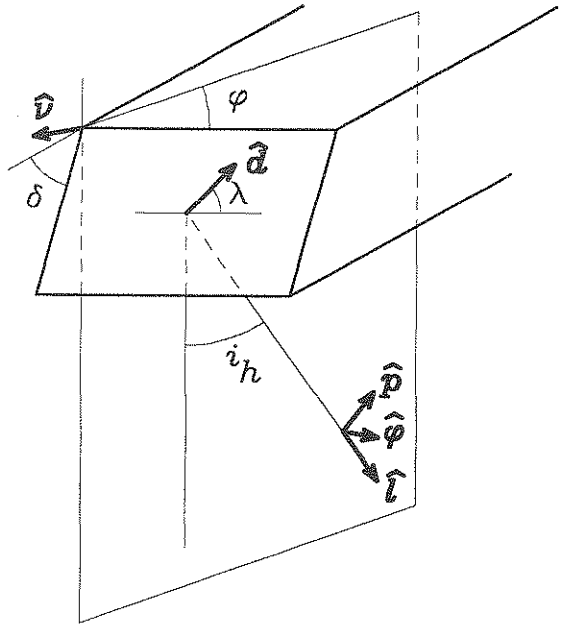

Fig. 2. Source geometry used in this paper. The fault representation is after KS76. The unit vector $\hat{\mathbf{d}}$ is in the direction of slip of the hanging block. It is defined by the dip angle δ and the slip angle λ. ϕ is the azimuth to the station, measured counterclockwise from the strike of the fault. $\hat{\nu}$ is the unit vector normal to the fault plane. The ray leaves at the take-off angle i_h in the vertical plane containing the great circle to the station; $\hat{\mathbf{l}}$, $\hat{\mathbf{p}}$ and $\hat{\boldsymbol{\phi}}$ are the unit vectors for the displacements $\mathbf{u}^P$, $\mathbf{u}^{SV}$ and $\mathbf{u}^{SH}$, respectively (after AR80).

ing the receiver), but AR80 orient $\mathbf{u}^{SV}$ with a positive component upwards in the plane of incidence (their Figure 4.20 p. 114), which amounts to $\mathbf{u}^{SV}$ positive towards the source upon reaching the receiver, whereas KS76 orient $\mathbf{u}^{SV}$ positive away from the source. Similarly, AR80 orient $\mathbf{u}^{SH}$ positive to the right as one reaches the receiver along the great circle path, whereas KS76 orient it positive to the left. In both cases the frame $\mathbf{u}^P$, $\mathbf{u}^{SV}$, $\mathbf{u}^{SH}$ remains direct.

These radiation coefficients have also been given for individual moment tensor components. AR80's Equations (4.84 to 4.86; p. 115) are particularly illustrative of the physical nature of the radiation pattern: it can easily be shown that the three coefficients R^P, R^{SV} and R^{SH} can be written simply as:

$$\begin{aligned} R^P &= < \hat{\gamma}\, \hat{\mathbf{M}}\, \hat{\gamma} > \\ R^{SV} &= < \hat{p}\, \hat{\mathbf{M}}\, \hat{\gamma} > \\ R^{SH} &= < \hat{\phi}\, \hat{\mathbf{M}}\, \hat{\gamma} > \end{aligned} \qquad (3)$$

where $\hat{\mathbf{M}} = \hat{\nu}\hat{d} + \hat{d}\hat{\nu} = \mathbf{M}_0 / M_0$ is the "directional" moment tensor of the source. The direction of slip $\hat{d}$ is defined as $\hat{d} = \underline{u}/u$; $\hat{\nu}$ is the unit vector normal to the fault plane. A product such as $\hat{c} = \hat{\nu}\hat{d}$ means the second-order tensor obtained as $c_{ij} = \hat{\nu}_i \hat{d}_j$, and corresponds in matrix terminology to right-multiplying $\hat{\nu}$ by the transposed of $\hat{d}$; the scalar product of the two vectors would correspond to left-multiplication. We call $\hat{\mathbf{M}}$ a "directional" moment tensor to emphasize that it is scaled, so that its eigenvalues are -1, 0, and +1, and as such carries information on the orientation of $\mathbf{M}_0$ in space, not on its actual amplitude, which would be related to the size of the earthquake. As such, $\hat{\mathbf{M}}$ is comparable to a *unit* vector such as $\hat{\nu}$; we do not use however the term "unit moment tensor", which is usually reserved for the Kronecker tensor δ_{ij}.

The vector $\hat{\gamma}$ is the unit vector in the direction of the departing ray. In a homogeneous medium, it is equivalent to $\hat{\mathbf{I}}$. We use circumflexes (^) on all unit vectors and directional tensors to highlight their character.

In other words, the radiation pattern of the source in the direction $\hat{\gamma}$ is described by the operator $\hat{\mathbf{M}}$ applied onto the unit vector $\hat{\gamma}$: the resulting vector $\mathbf{V}$, is proportional to $\alpha^3\, \mathbf{u}^P + \beta^3\, \mathbf{u}^S$, and can be regarded as a combined radiation of seismic motion in the direction $\hat{\gamma}$. In turn, projecting this vector onto the frame $\{\hat{\gamma}, \hat{p}, \hat{\phi}\}$ of the departing ray gives the three coefficients in their classical form. This interpretation is also given in AR80.

While moment tensor formalism may be more satisfactory from the analytical point of view, formulæ such as KS76's (A-12 to A-14) are more readily applicable to the familiar visualization of focal mechanisms through the strike, dip and slip angles (ϕ, δ, λ as defined on Figure 2).

Equation (3) reflects the perfect symmetry of the seismic source with respect to $\hat{d}$ (slip) and $\hat{\nu}$ (normal to the fault), illustrating the classical ambiguity between the two possible mechanisms corresponding to the same moment tensor. Also, the vector V obviously vanishes in the direction of the null axis, in which neither *P* nor *S* waves are radiated. Finally Equation (3) can of course be generalized to the case of non double-couple sources: for example, one would verify immediately that an explosion ($\mathbf{M}_0$ isotropic) generates no *S* waves.

GEOMETRICAL SPREADING

Geometrical spreading reflects the fact that the Earth is of spherical shape and radially heterogeneous. As such, the wavefront no longer has spherical symmetry when it reaches the receiver. As given by KS76, the geometrical spreading for *P* waves in a spherically symmetric Earth takes the form

$$g(\Delta) = \left(\frac{\rho_h \alpha_h}{\rho_0 \alpha_0} \cdot \frac{\sin i_h}{\sin \Delta} \cdot \frac{1}{\cos i_0} \left| \frac{d i_h}{d \Delta} \right| \right)^{1/2} \qquad (4)$$

This expression is derived by writing that the energy flux is conserved along ray tubes between a small sphere (of radius r_h) surrounding the source, and the wave front at the Earth's surface (see Figure 3). The volume density of kinetic energy is in both cases $k = \frac{1}{2}\rho u^2 \omega^2$, and the energy flux across a wavefront of area dS is $k \cdot \alpha \cdot dS$. In the vicinity of the hypocenter, the wave's amplitude u_h is proportional to r_h^{-1} (see Equation (2)) and dS_h is r_h^2 times the solid angle $2\pi \sin i_h \cdot |\, d i_h \,|$. In the vicinity of the Earth's surface, the cross-section of wavefront is $dS_0 = 2\pi a \sin\Delta \cdot a \; |\, d\Delta \,| \cos i_0$. Hence

$$\begin{aligned} &2\pi\, \rho_h \alpha_h\, r_h^2 \sin i_h \cdot |\, d i_h \,| \cdot u_h^2 \\ &\qquad = 2\pi\, \rho_0\, \alpha_0\, a^2 \sin\Delta \cos i_0 \; |\, d\Delta \,| \cdot u_0^2 \end{aligned} \qquad (5)$$

In other words the factor $\frac{1}{r_h}$ in Equation (2) giving u_h near the source must be replaced by $g(\Delta)/a$ (g given by (4) and a being the radius of the Earth), in order to obtain u_0 at the receiver. An alternate derivation of this result is given by Ben-Menahem and Singh (1981; p. 459). These authors call $G = g/a$ the "divergence coefficient" and tabulate it, in the case of *P* waves for a deep source and a receiver at the crust-mantle interface. As discussed by KS76 [p. 321], $g(\Delta)$ does not vary drastically

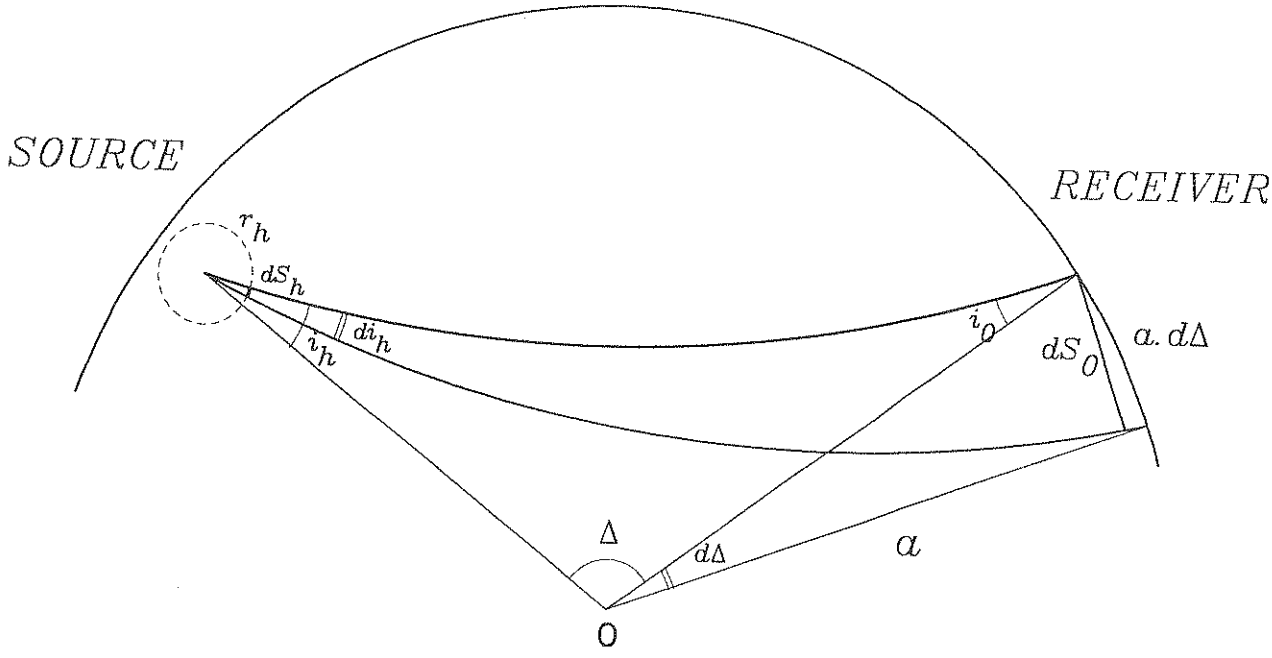

Fig. 3. Geometrical spreading of a teleseismic body wave. This figure considers two neighboring rays traveling to distances Δ and $\Delta + d\Delta$, with hypocentral take-off angles i_h and $i_h + di_h$ (note that di_h is negative). The energy flux across the small element (shown as a fat segment) dS_h of the focal sphere of radius r_h is equal to the flux across the section dS_0 of the wave front at the receiver end.

between distances of 30° and 90°, for a shallow source, and of a surface receiver. The above formula also has interesting applications in the vicinity of mantle triplications (Julian and Anderson, 1968) and when considering the decay of seismic waves with distance in other planets such as Mars or the Moon.

Equations (2) and (4) are often combined, resulting in expressions such as (4.88-90) of AR80, which involve the combination $[\rho_h^{1/2}\rho_0^{1/2}\,\alpha_h^{5/2}\alpha_0^{1/2}]$ in the denominator. The physical origin of the various exponents is best understood by separating back the various terms into (2) and (4).

The geometrical spreading of S waves is obtained from (4) by replacing the compressional velocities α by their shear counterparts β, and the incident angles i by the corresponding values of j. Assuming that the Poisson ratio of the Earth does not vary with depth, the two coefficients are equivalent in all geometries.

ANELASTIC ATTENUATION

The effect of anelastic attenuation is usually described in terms of a quality factor Q for the relevant body phase. The spectral amplitude of the body wave must be multiplied by the attenuation term

$$\exp\left[-\frac{\omega\tau}{2Q}\right] \qquad (6)$$

where τ is the travel time of the phase. Because of the general increase of Q with depth, it has been found empirically that $t^* = \tau/Q$ remains practically independent of distance, taking the values 1 s for teleseismic P waves and 4 s for S waves (Carpenter and Flinn, 1965; Anderson and Hart, 1978). More generally, and assuming that bulk attenuation can be neglected in the Earth's mantle, one would find that along identical paths,

$$Q^P = \frac{3}{4}\,\frac{\alpha^2}{\beta^2}\,Q^S \qquad (7)$$

the factor 3/4 stemming from the expression $\rho\alpha^2 = K + \frac{4}{3}\mu$. In turn, this leads to:

$$[\tau/Q]^P = \frac{4}{3}\,\frac{\beta^3}{\alpha^3}\,[\tau/Q]^S \qquad (8)$$

i.e., $t^{*P}/t^{*S} = 0.26$ for a Poisson solid, in good agreement with the observed numbers. In other words, S wave attenuation is on the average the fourth power of that of P waves. For typical

long-period body waves (with periods around 20 s), the difference in attenuation between P and S waves will only be a factor of about 2.5 . Since the S waves start off 5 times larger than P, they are still very prominent in the record (and often times larger than P). On the other hand, at short periods (1 s) the amplitude of S waves is reduced on average to 1/1000 that of the corresponding P wave. In practice, short period S waves are difficult to use at teleseismic distances. Their prominent observation results from exceptional circumstances, such as deep sources located below the low-velocity zone (where most of the attenuation takes place), and a receiver located above a shield (where the LVZ is poorly if at all developed).

The application of an attenuation function of the type (6) in the frequency domain is equivalent to the convolution of the time-domain synthetic with an attenuation operator

$$Q(t, Q, \tau) = \frac{1}{\pi} \cdot \frac{\tau/2Q}{t^2 + \tau^2/4Q^2} = \frac{2}{\pi} \cdot \frac{t^*}{t^{*2} + 4t^2} \qquad (9)$$

This absorption operator is, however, non-causal, which reflects the fact that the assumption of a constant group time τ in (6) is an oversimplification; as a result, more complex expressions of the operator Q are often used.

CONTRIBUTION OF THE DEPTH PHASES

The amplitude of a depth phase, say pP, is itself controlled by the same terms as for the primary wave P. Following KS76's notation, we should differentiate between properties at the hypocenter (indexed with the subscript h) and those at the surface, indexed with 0. However, in order to ease the physical discussion, we will consider shallow sources for which the structural properties (and hence the incidence angles) can conveniently be taken as equivalent at the two locations. We discuss later some problems arising from the case of deeper sources.

The excitation by the source of the upgoing ray in a depth phase is given by an expression similar to (2) and poses no special problems, the radiation pattern coefficients being simply evaluated in the appropriate directions ($\pi - i$, ϕ for pP; $\pi - j$, ϕ for sP). Because most sources are usually very shallow, the anelastic attenuation of pP (and sP) can be conveniently equaled to that of P, which amounts to ignoring the attenuation along the short upgoing ray. We concentrate therefore on the reflection coefficients and geometrical spreading, which must be examined with caution, especially in the case of the converted rays sP and pS.

In particular, the correct amplitude of a converted phase such as sP or pS is not simple to write, since the reflection takes place close to the source, and thus the upgoing wave cannot be regarded as a plane wave. On the other hand, the curvature of the Earth can usually be neglected in the vicinity of the source, and the problem becomes Lamb's problem, as solved by Cagniard (1939), de Hoop (1960), Helmberger (1974) and others, and presented in AR80 [Chapter 6]. Our purpose is not to repeat their analysis, nor to present a review of the Cagniard–de Hoop method, but simply to point out the fundamental steps of the computation, identifying along the way five factors which control the eventual amplitude of the reflected waves.

The basic philosophy of the Cagniard–de Hoop method is as follows: reflection coefficients are easily computed only for plane waves, but point sources generate spherical waves. Thus the incident spherical wave is first expanded into an integral of [real and complex] plane waves (the Weyl integral), and the reflected wave obtained by integrating back the plane waves, each weighted by the appropriate reflection coefficient (the "Cagniard integral"). The success of the method stems from the fact that under some approximations whose conditions of validity are not too stringent in the far field, the resulting integral can be approximated by a spherical wave.

Specifically, we start with the potential of the incident spherical wave (Φ for a P wave; Ψ for S), and expand it into plane waves through Weyl's integral (AR80 6.4). Clearly all reflection and transmission coefficients depend only on the magnitude of the horizontal wavevector ($k_r = (k_x^2 + k_y^2)^{1/2}$), not on its direction. Thus, it is possible to regroup plane waves with the same k_r, leading to Sommerfeld's integral (AR80 6.11)

$$\Phi = \frac{\exp[i\omega(\frac{r}{\alpha} - t)]}{4\pi\rho\alpha^2 r} \qquad (10a)$$

$$= \frac{i\omega}{4\pi\rho\alpha^2} e^{-i\omega t} \int_0^\infty \frac{p}{\xi} J_0(\omega p r') \exp(i\omega\xi \mid z - z_0 \mid) dp$$

where $\xi = \sqrt{\alpha^{-2} - p^2}$, in the case of an upgoing P wave, and

$$\Psi = \frac{\exp[i\omega(\frac{r}{\beta} - t)]}{4\pi\rho\beta^2 r} \qquad (10b)$$

$$= \frac{i\omega}{4\pi\rho\beta^2} e^{-i\omega t} \int_0^\infty \frac{p}{\eta} J_0(\omega p r') \exp(i\omega\eta \mid z - z_0 \mid) dp$$

where $\eta = \sqrt{\beta^{-2} - p^2}$, in the case of an upgoing S wave. At real incidences, one has simply $\xi = \cos i/\alpha$ and $\eta = \cos j/\beta$.

The integration is taken over the ray parameter $p = \frac{k_r}{\omega}$. The notation is that of AR80, except that, in keeping with Equation (2), the radius of the spherical polars is r (as opposed to R in AR80), and the radius of the cylindrical polars ($\sqrt{x^2 + y^2}$) is written r' (as opposed to r in AR80). Note that depending whether the ascending wave is p or s, the first factor in the potential is either $1/\rho\alpha^2$ or $1/\rho\beta^2$; the second factor is either $1/\xi$ or $1/\eta$. These two terms go hand in hand.

Each of these plane waves is then "weighted" by the appropriate reflection coefficient (for potential amplitudes). This introduces a third factor Π^{AB} where A and B are appropriate combinations of P and S in the notation of KS76. In the vicinity of the surface, the absolute values in (10) take the form $(z - z_0)$ $(z_0 < 0)$ for the incident waves, and the phase of reflected waves, now propagating downwards, involve the term $-i\omega\xi z$ (for an emerging P wave). The potential for pP will therefore be:

$$\Phi^{pP} = \frac{i\omega}{4\pi\rho\alpha^2} e^{-i\omega t} \cdot \int_0^\infty \frac{p}{\xi} \Pi^{PP} J_0(\omega p r') \exp -i\omega\xi(z + z_0)\, dp \qquad (11a)$$

and that for sP:

$$\Phi^{sP} = \frac{i\omega}{4\pi\rho\beta^2} e^{-i\omega t} \cdot \int_0^\infty \frac{p}{\eta} \Pi^{SP} J_0(\omega p r') \exp -i\omega(\xi z + \eta z_0)\, dp \qquad (11b)$$

Then, the integral over p is performed back, along a convenient contour in the complex plane.

In general, because the reflection coefficients Π are not constant, one does not reconstruct a true spherical wave (this would be the case however, for the SH problem, for which $\Pi = 1$ identically). It can be shown that the leading contributions to the resulting integrals are obtained for the values of the ray parameter p rendering the complex phase in (11) stationary. These values of p are simply the ray parameters of pP (or sP) in geometrical optics. The amplitude of the corresponding contribution can be evaluated by a variety of methods, notably the saddle-point approximation, which is most easily performed by changing, in the Cagniard integral, from the variable p to the phase

$$\omega\tau = \omega \left[p\, r' + \xi\, z_0 + \xi\, z \right] \qquad (12)$$

or

$$\omega\tau = \omega \left[p\, r' + \eta\, z_0 + \xi\, z \right]$$

respectively for pP and sP. This results in an additional (fourth) factor $dp/d\tau$. If the wave is not converted upon reflection, $dp/d\tau$ is simply proportional to the variable ξ (for pP; η for sS); if the wave is converted, $dp/d\tau$ does not have a simple analytical expression as a function of the source and receiver coordinates. However, at receiver depths either small or large compared to that of the source ($z \ll$ or $\gg z_0$ in (11)), one can neglect the contribution of the descending (resp. ascending) ray to the travel time, and thus $dp/d\tau$ becomes proportional to ξ (for pS close to the surface or sP at great depths) or η (for sP close to the surface or pS at great depths). A teleseismic wave corresponds to very large receiver depths in Lamb's problem, so that $dp/d\tau$ simply reflects the emerging wave, the fourth factor being ξ for pP and sP; η for pS and sS. In a sense, this factor involving the recomposition of plane waves into a (pseudo-) spherical wave, is the inverse of the second factor ($1/\xi$ or $1/\eta$) stemming from Sommerfeld's integral. If the nature of the wave is unchanged upon reflection (pP or sS), the second and fourth factors cancel out exactly; if a conversion takes place (sP or pS), they don't.

At this point, Cagniard-de Hoop's theory shows that the potential of the emerging wave "looks like" that of a spherical wave, appropriately lagged in time, and modulated in amplitude by the four factors listed above. This is only true for times t close to the geometrical arrival time, and is thus a high-frequency approximation. The final step consists of going from potential to displacements, keeping only the high-frequency terms, *i.e.*, introducing a fifth factor $1/\alpha$ or $1/\beta$, depending whether the emerging wave is P or S.

In conclusion, at a large distance from the source and the reflection point, a reflected wave such as sP can, for practical purposes, be computed as if it were a spherical P wave, phase-lagged according to the geometrical travel-time along the ray, and with an amplitude controlled by the five factors discussed above.

Table 1 gives the value of the five individual factors in all 4 cases of depth phases (pP, sP, pS and sS^{SV}), as well as the overall amplitude, relative to the direct wave. These must be multiplied by the appropriate radiation pattern coefficients and time-lagged source time functions (*e.g.*, $R^{SV}(\pi - j; \phi)$ and $\dot{X}(t - \tau^{sP})$ for sP), and they can then be combined with the direct wave (for example $R^P(i; \phi)\, \dot{X}(t - \tau^P)$ for direct P). It is easy to verify that our results for pP and sP are equivalent to KS76's Equation (8), given that these authors had considered a Poisson solid for which

Table 1
Summary of Factors Contributing to the Generalized Reflection Coefficients of Depth Phases

Phase	*pP*	*sP*	*pS*	*sS*
Original Potential	$\frac{1}{4\pi\rho\alpha^2}$	$\frac{1}{4\pi\rho\beta^2}$	$\frac{1}{4\pi\rho\alpha^2}$	$\frac{1}{4\pi\rho\beta^2}$
Sommerfeld's Expansion	$\frac{1}{\xi}$	$\frac{1}{\eta}$	$\frac{1}{\xi}$	$\frac{1}{\eta}$
Reflection Coefficient	$\Pi^{PP}(i)$	$\Pi^{SP}(j)$	$\Pi^{PS}(i)$	$\Pi^{SS}(j)$
dp/dτ at saddle point	ξ	ξ	η	η
Displacement from potential	$\frac{1}{\alpha}$	$\frac{1}{\alpha}$	$\frac{1}{\beta}$	$\frac{1}{\beta}$
Overall amplitude relative to direct wave	$\Pi^{PP}(i)$	$\frac{\alpha}{\beta}\Pi^{SP}(j)\frac{\cos i}{\cos j}$	$\frac{\beta}{\alpha}\Pi^{PS}(i)\frac{\cos j}{\cos i}$	$\Pi^{SS}(j)$

$\alpha/\beta = \sqrt{3}$. The case of *SH* polarization (their Equation (7)) is a trivial generalization of the last column of Table 1, since in this geometry, Π^{SS} is identically equal to 1.

It is important to stress that the reflection coefficients used in Table 1 are for *potentials*. If coefficients for *displacements* (such as listed, for example in AR80) are used, these formulæ must be adapted using the well known relations

$$\begin{aligned} \Pi^{PP} &= \grave{P}\acute{P} \\ \Pi^{SS} &= \grave{S}\acute{S} \\ \Pi^{SP} &= \frac{\alpha}{\beta}\grave{S}\acute{P} \\ \Pi^{PS} &= \frac{\beta}{\alpha}\grave{P}\acute{S} \end{aligned} \qquad (13)$$

this procedure amounting to combining the third and fifth factors in Table 1.

It is also important to realize that the above computation takes care of the geometrical spreading of the reflected phases: the conclusion of the Cagniard calculation is that, in the whole half-space, a reflected phase such as *sP* can be properly computed as if it were a regular *P* wave, appropriately time-lagged and weighted. Therefore the structure of the emerging reflected phase is correctly described by a *P* wave, modulated by the appropriate amplitude coefficient, and there is no need to compute a different geometrical spreading coefficient: $g(\Delta)$ for *P* can be factored into all three components (*P*, *pP* and *sP*).

At this point it is worth commenting on the occasional assertion that "spherical and plane waves have different reflection coefficients". This unfortunate language is a clear oversimplification of the problem. Note in particular that a spherical wave which is not converted (*pP* or *sS*) is reflected with the plane wave coefficient Π^{PP} or Π^{SS}.

A further note to check the results of Table 1

It is well known in normal mode theory that the excitation of both spheroidal and torsional modes goes to zero for a perfectly shallow source in the pure dip-slip geometry (perfectly vertical slip on a perfectly vertical fault plane). This result inhibits the resolution of two components of the moment tensor in the inversion of normal mode or surface wave spectra (Kanamori and Given, 1981). It is due to the fact that the relevant shear component of the eigenstress of the mode must vanish at the Earth's surface, and it applies to fundamentals and all overtones. A similar result should hold for body waves, since they can be considered a superposition of normal mode overtones. This is easily verified, for example in the case of *P* waves: in this particular geometry, the radiation patterns of direct *P*, *pP* and *sP* are simply (Equations (A-11) to (A-14) of KS76):

$$\begin{aligned} R^P &= -R^{pP} = \sin\phi \sin 2i_h \\ R^{sP} &= -\sin\phi \cos 2j_h \end{aligned} \qquad (14)$$

(we revert here to the fully indexed $i_h;j_h$ notation). When the source depth goes to zero, the time delays vanish, and the amplitude of the resulting wave is simply:

$$R^P + R^{pP}\cdot\acute{P}\grave{P}(i_h) + R^{sP}\cdot\acute{S}\grave{P}(j_h)\frac{\alpha^2\cos i_h}{\beta^2\cos j_h} \qquad (15)$$

AR80's formulæ (5.26-30) p. 140 can be used to verify that this expression vanishes identically, for all i_h and j_h satisfying Snell's law, and, of course, for all azimuths ϕ. Note that it is correct to use KS76's radiation pattern coefficients, and AR80's reflection coefficients, since the orientation convention for the latter (AR80's Figure 5.5b p. 139) is compatible with the Kanamori conventions (but not with the AR80 *source* conventions). A similar result is also obtained for the generalized *SV* wave, composed of *SV*, *pSV* and *sSV*. In this case, however, the AR80 coefficients $\acute{S}\grave{S}$ and $\acute{P}\grave{S}$ must be flipped, since the orientation convention of the *reflected S* wave is incompatible with KS76. The total amplitude of the generalized *SV* wave is thus:

$$R^{SV} - R^{pS} \cdot \acute{P}\grave{S}(i_h) \frac{\beta^2 \cos j_h}{\alpha^2 \cos i_h} - R^{sSV} \cdot \acute{S}\grave{S}(j_h) \qquad (16)$$

which, again, vanishes identically given

$$R^{SV} = R^{sSV} = -\sin\phi \cos 2j_h; \qquad (17)$$
$$R^{pS} = -\sin\phi \sin 2i_h$$

The case of *SH* is trivial since in the dip-slip geometry, $R^{SH} = -R^{sSH}$ and $\acute{S}\grave{S} = 1$ for *SH* polarization.

In conclusion, the perfectly shallow pure dip-slip geometry excites no seismic wave, body or surface. This exercise verifies, in particular, that the same geometrical spreading coefficient $g(\Delta)$ can be factored into the three components of the *P* wave. It also serves to illustrate the extreme care which must be given to orientation conventions when using excitation and/or reflection coefficients, even when obtained from different chapters of the same book.

SURFACE RESPONSE AT THE RECEIVER

This well-known term describes the fact that an incident seismic wave undergoes reflection and conversion at the surface even as it is being recorded, and that therefore seismic records will render the full motion of the Earth, *i.e.*, the combination of not only the incident wave, but also the reflected and converted ones (Gutenberg, 1952; Nuttli, 1961). This classical effect is easily computed from the expression of the reflection coefficients of plane waves at a free boundary. In the notation of AR80 (p. 140), the response of a vertical seismometer to an incident *P* wave of unit amplitude will be

$$C^P(i_0) = [\,1 - \acute{P}\grave{P}(i_0)\,] \cos i_0 + \acute{P}\grave{S}(i_0) \sin j_0 \qquad (18)$$
$$= \frac{\frac{2}{\beta^2}\left(\frac{1}{\beta^2} - 2p^2\right)\cos i_0}{\left(\frac{1}{\beta^2} - 2p^2\right)^2 + \frac{4p^2 \cos i_0 \cos j_0}{\alpha\beta}}$$

while the response of a horizontal seismometer polarized away from the source to an incident *SV* wave of unit amplitude will similarly be

$$C^{SV}(j_0) = [\,1 + \acute{S}\grave{S}(j_0)\,] \cos j_0 + \acute{S}\grave{P}(j_0) \sin i_0 \qquad (19)$$
$$= \frac{\frac{2}{\beta^2}\left(\frac{1}{\beta^2} - 2p^2\right)\cos j_0}{\left(\frac{1}{\beta^2} - 2p^2\right)^2 + \frac{4p^2 \cos i_0 \cos j_0}{\alpha\beta}}$$

The response of a transversely (*SH*) polarized seismometer to an incident *SH* wave of unit amplitude is always $C^{SH} = 2$.

Finally, the horizontal motion of an incident *P* wave is given by

$$C_H^P(i_0) = \frac{\frac{4p}{\beta^3}\cos i_0 \cos j_0}{\left(\frac{1}{\beta^2} - 2p^2\right)^2 + \frac{4p^2 \cos i_0 \cos j_0}{\alpha\beta}} \qquad (20)$$

and the vertical motion due to an incident *SV* wave by:

$$C_Z^{SV}(j_0) = \frac{-\frac{4p}{\alpha\beta^2}\cos i_0 \cos j_0}{\left(\frac{1}{\beta^2} - 2p^2\right)^2 + \frac{4p^2 \cos i_0 \cos j_0}{\alpha\beta}} \qquad (21)$$

Note that these equations are identical to the formulæ proposed in Problem 5.6 of AR80 (p.190), given that these authors have oriented the vertical axis downwards. Also, note that while (18) and (19) may look rather similar, their behavior with incidence is quite different since at large incidences, the reflection of *S* becomes post-critical for the converted *SP* wave, strongly affecting the amplitude (and the phase) of C^{SV}. Their behavior for a Poisson solid is given on Figure 4.

Equations (18-22) have many applications, notably in allowing the correct interpretation of the incidence angle of a *P* wave from a three-component recording of its first motion. Similarly, and as discussed by Nuttli and Whitmore (1962), an apparent *SV/SH* amplitude ratio must be corrected to take into account $C^{SV}(j_0)$ before it can yield any information regarding the combined source-receiver geometry. Figure 4 shows that due to the onset of critical reflection, *SV/SH* ratios become very unreliable for incidence angles $j_0 \geq 30°$. In particular, at the greater range of incidences, the phase of $C^{SV}(j_0)$ approaches π, which means the polarity of *SV* appears fully reversed.

Even though the above formalism appears very straightforward, a major problem when applying it in real life is that of defining an

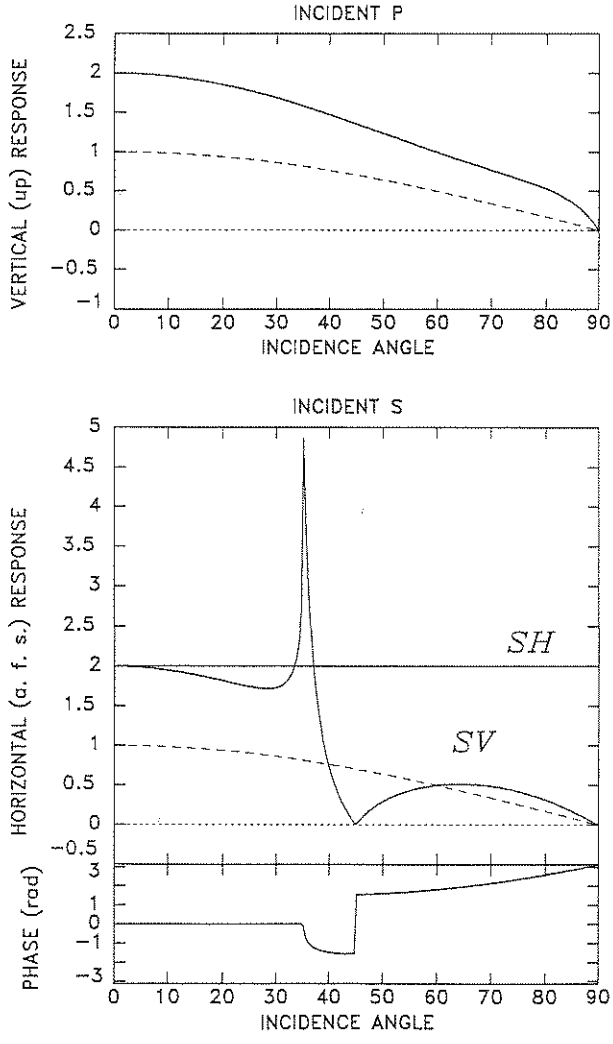

Fig. 4. Surface response coefficients $C^P(i_0)$ and $C^S(j_0)$ as a function of the incidence angle and in the case of a Poisson solid, as described by Equations (18) and (19). *Top:* Response of a vertical seismometer to an incident P wave of unit amplitude. The solid line represents C^P, the dashed one ($\cos i_0$) the contribution of the incident P alone. *Bottom:* Response of a horizontal seismometer polarized away from the source, to an incident SV wave of unit amplitude. The solid curves show the amplitude (top frame) and phase (bottom frame) of C^{SV}. Note that due to critical $S \rightarrow P$ reflection, this coefficient becomes complex around $j_0 = 35°$. C^{SV} is also compared to the surface response for SH waves (identically equal to 2), and to the contribution of the incident wave alone ($\cos j_0$; dashed line). This figure shows that the apparent SH/SV ratio is strongly distorted beyond 30° of incidence.

appropriate incidence angle. When dealing with a layered crust, the incidence angle can vary sharply over the last few km of propagation, resulting in what amounts to a frequency-dependent surface response. For example, the analysis of the 3-component motion of an incident P wave usually yields a reasonable estimate of the azimuth of arrival, but the incidence angle (which in principle could give an estimate of the distance) remains generally imprecise. In more general terms, the response of a layered medium, such as a typical crust-over-mantle structure, to an incident body wave, has been studied in great detail by Haskell (1960, 1962).

THE CASE OF DEEP SOURCES

The above algorithm was developed and used extensively to compute synthetic seismograms from sources located in the crust or in the shallowest parts of the upper mantle (see for example Stein and Wiens, 1986). In principle, it should be possible to extend it to deeper sources. We discuss below a number of problems which become relevant for intermediate and/or deep sources.

1. In theory, it is no longer possible to neglect the curvature of the Earth when computing the amplitudes of pP and sP by the Cagniard-de Hoop method (the assumption that P, pP and sP share a common ray parameter becomes inaccurate). In addition, precursors to pP resulting, for example from underside reflections at the Moho discontinuity, will be present. In general, the contributions with the largest amplitudes remain pP and sP, but their time lags with respect to direct P will depart from their expressions in the flat-layered problem. One way to handle this situation is to carry out a so-called "Earth flattening transformation" (Chapman, 1973) before setting up the Cagniard problem.
2. A further limitation involves the assumption that the receiver is very much farther away from the reflection point than the source. This approximation helped us estimate $dp/d\tau$ in the Cagniard integral in the case of converted waves, and may break down at the shorter range of epicentral distances. Note that both of the above problems (1. and 2.) are sensitive at distances close to the initiation of the depth phases, and disappear at larger distances.
3. The attenuation operator has to be carefully selected, and occasionally fine-tuned to the particular path studied. Because most of the attenuation in the Earth's mantle takes place in the low-velocity zone (Anderson and Hart, 1978), direct P or S rays leaving from a source below the LVZ will be significantly less attenuated. As discussed by Burdick (1978), t^* values of 0.75 s for P waves and 2.5 s for S waves are adequate for sources deeper than 200 km. On the opposite, a reflected ray, such as pP or sS will be subject to an additional episode of attenuation as it travels up through the upper mantle. Different Q operators must then be used for the three components of Equation (1), and the convolutions performed inside the bracket. The situation is made even more complex by the strong lateral heterogeneity existing in the vicinity of all deep seismic sources: an upgoing ray traveling inside the cold slab, will be less attenuated than the same phase to a different station, which may travel through the hot mantle just above the slab (Utsu, 1971). While this strongly affects short-period arrivals, it can also influence the relative amplitudes of long-period P, pP and sP.
4. Other phases can arrive between P and pP, such as PcP, or between pP and sP, such as $pPcP$ or PP. These phases have to be computed independently if the whole seismogram is to be modeled.

ACKNOWLEDGMENTS

I thank my students over the years for motivating many reflections on body wave synthetics. I benefited from discussions with Aristeo Pelayo, and from constructive criticism from an anonymous reviewer.

REFERENCES

Aki, K., and P.G. Richards (1980). *Quantitative Seismology*, Freeman, San Francisco, 2 vol., 932 pp.

Anderson, D.L., and R.S. Hart (1978). Attenuation models of the Earth, *Phys. Earth Planet. Int.* **16**, 289-306.

Ben-Menahem, A., and S.J. Singh (1981). *Seismic Waves and Sources*, Springer-Verlag, New York, 1108 pp.

Burdick, L.J. (1978). t^* for S waves with a continental ray path, *Bull. Seism. Soc. Am.* **68**, 1013-1030.

Cagniard, L. (1939). *Réflection et réfraction des ondes sismiques progressives*, Gauthier-Villars, Paris, 255 pp.

Carpenter, E.W., and E.A. Flinn (1965). Attenuation of teleseismic body waves, *Nature* **207**, 745.

Chapman, C.H. (1973). The Earth-flattening transformation in body-wave theory, *Geophys. J. Roy. astr. Soc.* **35**, 55-70.

Chapman, C.H. (1978). A new method for computing seismograms, *Geophys. J. Roy. astr. Soc.* **54**, 481-518.

de Hoop, A.T. (1960). A modification of Cagniard's method for solving seismic pulse problems, *Appl. Sci. Res.* **B8**, 349-356.

Fuchs, K., and G. Müller (1971). Computation of synthetic seismograms with the reflectivity method and comparison of observations, *Geophys. J. Roy. astr. Soc.* **23**, 417-433.

Gutenberg, B. (1952). *SV* and *SH*, *Trans. Am. Geophys. Un.*, **33**, 573-584.

Haskell, N.A. (1960). Crustal reflection of plane *SH* waves, *J. Geophys. Res.* **65**, 4147-4150.

Haskell, N.A. (1962). Crustal reflection of plane *P* and *SV* waves, *J. Geophys. Res.* **67**, 4751-4767.

Helmberger, D.V. (1968). The crust-mantle transition in the Bering Sea, *Bull. Seism. Soc. Am.* **58**, 179-214

Helmberger, D.V. (1974). Generalized ray theory for shear dislocations, *Bull. Seism. Soc. Am.* **64**, 45-64.

Kanamori, H., and J.W. Given (1981). Use of long-period surface wave for rapid determination of earthquake source parameters, *Phys. Earth Planet. Inter.* **27**, 8-31.

Kanamori, H., and G.S. Stewart (1976). Mode of the strain release along the Gibbs Fracture Zone, Mid-Atlantic Ridge, *Phys. Earth Planet. Inter.* **11**, 312-332.

Julian, B.R., and D.L. Anderson (1968). Travel times, apparent velocities and amplitudes of body waves, *Bull. Seism. Soc. Am.*, **58**, 339-366.

Langston, C.A., and D.V. Helmberger (1975). A procedure for modeling shallow dislocations sources, *Geophys. J. Roy. astr. Soc.* **42**, 177-130.

Nuttli, O.W. (1961). The effect of the Earth's surface on the *S* wave particle motion, *Bull. Seism. Soc. Am.* **51**, 237-246.

Nuttli, O.W., and J.D. Whitmore (1962). On the determination of the polarization angle of the *S* wave, *Bull. Seism. Soc. Am.* **52**, 95-107.

Stein, S., and D.A. Wiens (1986). Depth determination for shallow teleseismic earthquakes: Methods and results, *Revs. Geophys. Space Phys.* **24**, 806-832.

Utsu, T. (1971). Evidence for anomalous structures of island arcs, with special reference to the Japanese region, *Revs. Geophys. Space Phys.* **9**, 839-890.

Submitted September 24, 1991
Revised December 30, 1991
Accepted February 23, 1992